UNIVERSITY OF HELSINKI

https://helda.helsinki.fi

Sexual dimorphism in root exudation mediates belowground neighbor recognition and shapes rhizosphere soil microbial assembly

Guo, Qingxue; Chen, Xinyi; Duan, Jincheng; Korpelainen, Helena; Li, Chunyang

2026-08-02
Wiley Blackwell
http://hdl.handle.net/10138/640284
Guo, Q, Chen, X, Duan, J, Korpelainen, H & Li, C 2026, 'Sexual dimorphism in root exudation mediates belowground neighbor recognition and shapes rhizosphere soil microbial assembly', New Phytologist. https://doi.org/10.1111/nph.71486

Downloaded from Helda, University of Helsinki institutional repository. https://helda.helsinki.fi
This is an electronic reprint of the original article.
This reprint may differ from the original in pagination and typographic detail.
Please cite the original version.

The Revision for NPH-MS-2026-56001

Sexual dimorphism in root exudation mediates belowground neighbor recognition and shapes rhizosphere soil microbial assembly

Qingxue Guo [1,2], Xinyi Chen [1], Jincheng Duan [1], Helena Korpelainen [3], Chunyang Li [2,*]

[1] College of Life and Environmental Sciences, Hangzhou Normal University, Hangzhou 311121, China

[2] State Key Laboratory for Vegetation Structure, Function and Construction (VegLab), College of Agriculture and Biotechnology, Zhejiang University, Hangzhou 310058, China

[3] Department of Agricultural Sciences, Viikki Plant Science Centre, University of Helsinki, P.O. Box 27, FI-00014, Finland

[*]Corresponding author: Chunyang Li, licy12@zju.edu.cn

ORCID

Qingxue Guo: https://orcid.org/0000-0002-1812-8366

Helena Korpelainen: https://orcid.org/0000-0002-7046-6995

Chunyang Li: https://orcid.org/0000-0003-2895-2786

Running head: Belowground recognition and cooperative networks

Summary

- Sexual dimorphism in physiological traits is a hallmark of dioecious plants, yet the extent to which these sex-specific differences extend belowground to mediate neighbor recognition and the assembly of rhizosphere microbial communities remains largely unexplored.

- In this study, using an integrated experimental approach with the dioecious model *Populus cathayana*, we combined split-root experiments, ^{13}C-pulse labeling, and multi-omics to dissect the interactions between plant sex, root exudation, and microbiome assembly.

- We demonstrate that male and female plants discriminate and respond to the sexual identity of neighbors by modulating their root exudation profiles. Upon perceiving same-sex neighbors, females upregulated metabolically costly compounds, reflecting a defensive response to intense intraspecific competition. In contrast, under inter-sexual interactions, females shifted toward growth-promoting pathways, while males significantly increased allocation of newly fixed photosynthetic carbon to the rhizosphere. This male-driven carbon investment fostered highly interconnected cross-kingdom microbial networks with increased cooperative interactions. These microbial shifts directly enhanced nitrogen content and photosynthetic ability in females.

- Our findings demonstrate that sexual dimorphism in root exudation fosters cooperative soil microbial networks, providing a transformative framework for understanding how belowground sexual recognition enhances the ecological resilience and productivity of mixed-sex plant populations.

Keywords: Sexual dimorphism, sex recognition, microbiome assembly, root exudation, soil microbial legacy.

Introduction

Plant-soil interactions are fundamental drivers of terrestrial ecosystem processes and critical for the sustainability of forestry plantations. Central to these interactions is the chemical language of root exudates belowground, which orchestrates the dialogue between plants and soil microbiome (Henneron *et al.*, 2020; Jing *et al.*, 2023). The chemical profile and release rate of root exudates are extremely sensitive, modulated by plant identity, environmental stressors, and neighbor presence (Kong *et al.*, 2018; Ulbrich *et al.*, 2022). This chemical plasticity actively shapes the structure and function of soil microbial communities, creating soil microbial legacies that can facilitate or inhibit the growth of subsequent plants (Hannula *et al.*, 2021; Nannipieri *et al.*, 2023). While previous research has extensively documented how such chemical language varies between plant species to drive these feedbacks, the potential for intraspecific diversification, specifically the effects of male and female interactions within dioecious plants, to alleviate or alter these belowground processes remains largely unexplored.

In dioecious angiosperms, which account for approximately 5-6% of species, males and females frequently evolve divergent life-history strategies, particularly with respect to resource allocation to growth versus reproduction (Renner, 2014; Moutouama *et al.*, 2025). Females generally bear higher reproductive costs, which is often reflected in greater belowground carbon investment, larger root systems and altered root exudation patterns compared to males, whereas males may prioritize rapid resource acquisition and maintain a more stable root carbon sink to sustain their microbial partners (Hultine *et al.*, 2016; Xia *et al.*, 2022; Guo *et al.*, 2024). These sex-specific resource allocation strategies directly affect the quantity and composition of rhizodeposits, providing a mechanistic basis for why male and female plants can cultivate distinct soil microbiomes (Xia *et al.*, 2022; Guo *et al.*, 2023; Mao *et al.*, 2024). Because root exudates serve as the primary chemical interface between plants and the soil microbiome, understanding how sexual dimorphism in exudation shapes microbial communities is essential for explaining sex-mediated plant-soil feedbacks. While aboveground volatile organic compounds may also contribute to neighbor perception in dioecious plants, we focused here on belowground chemical signaling, which represents

the most direct pathway through which plants differentially recruit and maintain rhizosphere microbial assemblages.

Previous studies have shown that male and female plants can significantly influence one another's fitness when they coexist. For example, male plants have been shown to promote growth or improve the resistance abilities of female plants to unfavorable environments (Xia et al., 2022; Liu et al., 2024). By contrast, females often suffer severe negative impacts from female neighbors under unfavorable conditions (Guo et al., 2024; Liu et al., 2024). When a plant grows in soil conditioned by a predecessor, it responds to the existing microbial legacy while simultaneously remodeling that legacy through its own root exudates. The root exudates of a current plant growing in its own conditioned soil are probably different from those in soil conditioned by the opposite sex. These real-time modifications driven by the current plant's sex would contribute to the overall outcome of plant-soil interactions. However, a critical knowledge gap remains. Do plants actively perceive the sex of their neighbors and dynamically modulate their root exudation in response? How these neighbor-induced chemical dialogues override or synergize with pre-existing soil microbial legacies? Such belowground sex discrimination could allow individuals to adjust their competitive or facilitative strategies depending on the sexual identity of their neighbors, with profound consequences for microbiome assembly and plant performance.

Poplars (*Populus* spp.) are globally distributed dioecious trees and widely used in forestry (Sloan & Sayer, 2015; Fang *et al.*, 2021). Here, using the dioecious tree *Populus cathayana* as a model, we conducted a series of integrated experiments to dissect this sex-specific dialogue from the mechanism to ecological consequences. Specifically, we aimed to answer three key questions: (1) Do male and female poplars generate distinct soil microbial legacies that differentially affect plant physiology? (2) Do these plants exhibit belowground sexual recognition, altering their root exudate profiles in response to same-sex versus opposite-sex neighbors? (3) Is this neighbor-induced chemical plasticity a direct driver

of shifts in the soil microbial community? By addressing these questions, we sought to provide the first comprehensive evidence for a sophisticated, chemically-mediated recognition system between sexes in plants and its cascading effects on the soil microbiome.

Materials and Methods

Study site and soil collection

The study utilized soils collected from the Xuanhua County Plain (40°25' N, 115°2' E) in the Hebei Province, China. This region is characterized by a semiarid climate, with a mean annual precipitation of 400.3 mm, an evaporation rate of 1,862.5 mm, and a mean annual temperature of 7.6 °C (Ren *et al.*, 2021). The area is typified by aeolian sandy soil and has experienced significant land degradation due to wind erosion and deposition. To prevent further environmental deterioration and restore degraded lands, poplar plantations (*P. cathayana*) have been widely established in this region. The plantations were originally established with a highly diverse pool of cuttings, with over 200 male and over 200 female parent trees sampled in the surrounding mountains. This ensured a broad genetic base in the mature plantation, from which we sourced our experimental plants. The traits of degraded soils are pH 8.82, soil organic matter 5.9 g kg^{-1}, dissolved organic carbon 31.59 mg kg^{-1}, total nitrogen 0.3 g kg^{-1}, total phosphorus 0.33 g kg^{-1}, and available phosphorus 5.80 mg kg^{-1}. For this study, degraded soils were collected from unplanted areas to serve as the initial substrate and they were transported to the laboratory at the Hangzhou Normal University for subsequent experiments.

Plant material and soil conditioning

The sexual identity of *P. cathayana* individuals was determined based on floral morphology during the spring flowering season. One-year-old cuttings of both sexes were collected from a local *P. cathayana* plantation (Guo *et al.*, 2024). To generate sex-specific soil leg-

acies, a soil conditioning phase was conducted. Crucially, to generate sex-specific soil legacies, each cutting was taken from a different mother tree. These cuttings were grown individually in plastic pots (33 cm height, 56 cm diameter) filled with homogenized degraded field soil for two years. Following this two-year conditioning phase, the soils were designated as 'male-conditioned soil' and 'female-conditioned soil', respectively.

To evaluate the response of *P. cathayana* to sex-specific soil microbial legacies, a microcosm experiment was conducted using window rhizoboxes (20 cm width × 40 cm height × 4 cm depth), as modified from Xia *et al.* (2023). Each rhizobox was filled with either male- or female-conditioned soil, and a 3-cm layer of sterilized sand was applied to the surface to minimize contamination from airborne microbes (Fig. 1A). To further ensure genetic independence, the experimental plants for the microcosms were cuttings taken from different mother trees, and were randomly assigned to each treatment. A fully factorial design was employed with two soil history types and two plant sexes, resulting in four treatments: (1) male in home soil (male-conditioned); (2) male in foreign soil (female-conditioned); (3) female in home soil (female-conditioned); and (4) female in foreign soil (male-conditioned). Initially, 20 replicate rhizoboxes were established for each treatment. One month after sprouting, 15 replicates per treatment were selected based on uniform growth performance for the subsequent experiment. Plants were irrigated with sterile water throughout the growth period to maintain soil moisture.

After three months of growth, ten replicates per treatment were selected for a ^{13}C-CO_2 pulse-labeling experiment. Five replicates were placed in a transparent plastic chamber for isotope labeling, while the other five served as unlabeled controls placed in a separate chamber to account for background ^{13}C abundance. Inside the labeling chamber, $^{13}CO_2$ was generated by reacting barium carbonate ($Ba^{13}CO_3$, 99.9%) with 2 M HCl. To maintain a relatively stable CO_2 concentration (900-1000 ppm) during the labeling period, additional CO_2 was generated using sodium carbonate (Na_2CO_3) and 2 M HCl (Liu *et al.*, 2024). The unlabeled control chamber was maintained at the same CO_2 concentration (900-1000 ppm)

using only Na_2CO_3. Fans were installed in both chambers to ensure uniform air circulation. The labeling was conducted from 8:30 to 12:30, after which the chambers were removed.

Rhizosphere soil was collected from both labeled (n = 5) and unlabeled (n = 5) plants three days after labeling. Prior to the destructive harvesting of the remaining five replicates, the net photosynthetic rate was measured. Plants were then harvested and separated into leaves, stems, and roots. Fresh roots were immediately scanned, and root architecture was analyzed using the WinRhizo system (Régent Instruments Inc., Québec, Canada). All plant tissues were oven-dried at 75 °C to determine biomass. Rhizosphere soil samples were divided into three subsamples: one portion was stored at -80 °C for DNA extraction and ^{13}C-PLFA analysis; one portion was stored at -20 °C for enzyme activity assays; and the final portion was air-dried for soil nitrogen (N) analysis.

Split-root soil choice

To further investigate the active foraging behavior and spatial root distribution of *P. cathayana* in response to sex-specific soil legacies, a root choice experiment was conducted. The same window rhizoboxes described above were utilized but modified to create a heterogeneous soil environment. Each rhizobox was divided into two distinct compartments using a central PVC barrier (37 cm length × 0.5 cm thickness). One compartment was filled with male-conditioned soil, while the adjacent compartment was filled with female-conditioned soil. As in the previous experiment, a 3-cm layer of sterilized sand was uniformly applied to the soil surface to minimize airborne microbial contamination. A single *P. cathayana* cutting (either male or female) was transplanted into the center of the rhizobox, positioned directly above the PVC divider. This arrangement allowed the developing root system to potentially access and forage in both soil types simultaneously. Ten replicate rhizoboxes were established for each plant sex. The ^{13}C-CO_2 pulse-labeling procedure was conducted following the protocol described above before harvest. Upon harvest, roots from the two separate compartments were carefully disentangled, washed, and immediately scanned to assess root architecture using the WinRhizo system. Rhizosphere

soil samples were collected separately from each compartment for ^{13}C-PLFA analysis and soil N determination.

Hydroponic reciprocal transfer

To investigate the plasticity of root exudates in response to the perceived sexual identity of neighbors, we designed a hydroponic reciprocal transfer experiment in a greenhouse (Fig. S1). Male and female cuttings were propagated in individual opaque plastic containers filled with Long Ashton nutrient solution (Luo *et al.*, 2015). After a one-month establishment period, 15 uniform individuals of each sex were selected and organized into pairs to create three distinct interaction scenarios (n = 5 pairs per scenario): inter-sexual interactions (one male paired with one female), and intra-sexual interactions (two females paired together, or two males paired together). The growth conditions were set as follows: a 12 h light/12 h dark photoperiod, relative humidity maintained at 60-65%, with temperature fluctuating between 27 °C during the light period and 25 °C during the dark period.

A continuous reciprocal transfer protocol was implemented to simulate neighbor recognition via root exudates. Specifically, each plant was grown in its individual container for 24 h to condition the solution with its own root exudates. Subsequently, the two plants within each pair were reciprocally transferred, i.e., plant A was moved into the solution conditioned by Plant B, and vice versa for a 24-h perception phase. After this 48-h cycle, the nutrient solution was replaced with fresh medium, and plants were returned to their original containers to begin the next cycle. Plants were carefully moved between containers by gently lifting the entire root system while submerged in the solution. This procedure was repeated continuously for 50 days. Following this treatment period, plants were carefully removed, roots were rinsed, and each plant was transferred to a glass container filled with 800 mL of ultrapure water to collect root exudates. The containers were wrapped in black plastic bags to exclude light. After 12 h of incubation, the exudates were collected and immediately stored at -80 °C. Prior to exudate collection, the net photosynthetic rate was measured, and plants were harvested and oven-dried to determine biomass.

Effects of root exudates on microbiota assembly

To investigate the ecological consequences of sex-specific root exudate plasticity on the rhizosphere microbiota assembly, we conducted a controlled exudate-addition experiment (Fig. S2). We established a separate cohort of 'donor' plants (10 males and 10 females) in opaque plastic containers filled with Long Ashton solution. The 10 male donor cuttings were sampled from 5 distinct mother trees (2 cuttings per tree), and the 10 female donors were collected in the same way. Starting one month after planting, root exudates were collected weekly following the previously described water-incubation protocol. To create five independent samples, the exudates from the two cuttings derived from the same mother tree were combined and stored at -20 ºC until use. Simultaneously, a soil microcosm experiment was established using window rhizoboxes (35 cm width × 50 cm height × 5 cm depth). To isolate the effect of exudates on the home soil microbiome, male cuttings were planted in male-conditioned soil, and female cuttings were planted in female-conditioned soil. The experiment employed a factorial design with each plant-soil system receiving one of the three irrigation treatments: (1) sterile water (Control), (2) pooled male root exudates (M-exu), or (3) pooled female root exudates (Fe-exu). Solutions were applied daily to the root zone, with volumes adjusted from 20 mL to 50 mL during the course of the experiment. Each of the six treatment combinations (2 plant-soil systems × 3 exudate treatments) was replicated five times. After three months of growth, plants were harvested and oven-dried at 75 °C for 72 h to measure biomass. Rhizosphere soil samples were collected immediately upon harvest and stored at -80 °C for subsequent DNA extraction.

Leaf photosynthetic rates were measured using a portable photosynthesis system (LI-6800, Li-Cor, USA). The N content and soil enzyme assays of β-1,4-glucosidase (BG), acid phosphatase (AP), polyphenol oxidase (POX) and peroxidase (PER) were determined according to the protocol described by Jing et al. (Jing et al. 2020). Soil PLFAs were extracted from 3.0 g of freeze-dried soil following a modified Bligh and Dyer method (Frostegård *et al.* 1993).

The soil microbial biomass was estimated by phospholipid fatty acid (PLFA) analysis following established procedures (Schindlbacher *et al.* 2011). Phospholipids were separated from neutral lipids and glycolipids via silicic acid chromatography and subsequently converted to fatty acid methyl esters (FAMEs) by mild alkaline methanolysis (White *et al.* 1979). The incorporation of ^{13}C into the PLFAs was calculated as in Zhang et al. (Zhang *et al.* 2019). Markers representing Gram-positive bacteria, Gram-negative bacteria and fungi were used (Willers *et al.* 2015; Luo *et al.* 2022). Non-specific PLFAs (14:0, 16:0, 17:0, 18:0, 20:0), present across a range of microorganisms, were also analyzed (Joergensen 2022). Root exudate profiles were tested with LC-MS. Details of all these measurements are provided in Supplementary Materials.

Soil genomic DNA was extracted using the ALFA-SEQ Magnetic Soil DNA Kit. After assessing the DNA concentration and purity, the bacterial 16S rRNA gene and fungal ITS region were amplified with the primer pairs 799F/1193R (Beckers *et al.* 2016) and ITS3-F/ITS4-R (McKay *et al.* 1999), respectively. Detailed amplification conditions are provided in the Supplementary Materials. Raw sequencing reads were quality-filtered, trimmed of primers, and merged. Amplicon Sequence Variants (ASVs) were generated by denoising the data, which included chimera removal. Taxonomic assignment for bacterial and fungal ASVs was performed against the SILVA and UNITE reference databases, respectively.

Statistical analysis

Independent Student's *t*-tests were employed to evaluate the effects of sex-specific soil legacies on plant growth, net photosynthetic rates, root architecture, soil enzyme activities, and ^{13}C-PLFA profiles. Data were checked for normality and homogeneity of variance prior to analysis. Microbial community analysis was primarily conducted using the 'microeco' package (Liu *et al.*, 2021). To identify specific bacterial and fungal biomarkers associated with sex-specific soil legacies, Linear Discriminant Analysis Effect Size (LEfSe) was performed (LDA threshold > 2.5).

Metabolomic data were analyzed using Orthogonal Partial Least-Squares Discriminant Analysis (OPLS-DA) to discriminate root exudate profiles between treatments. Variable Importance in Projection (VIP) scores were calculated to rank the contribution of each metabolite to group separation. Differential metabolites were identified based on the following criteria: VIP > 1.0, $p < 0.05$ (Student's *t*-test), and $|\log_2 FC| > 1.5$. Functional annotation of these metabolites was performed using the KEGG database. Specific comparisons of phenolic and terpenoid compound concentrations between sexes were conducted using independent Student's *t*-tests.

In the exudate-addition experiment, the beta-diversity was based on Bray-Curtis dissimilarity, and pairwise comparisons were tested using the Wilcoxon rank-sum test. To identify taxa with significant differential abundance between treatments, we used the 'DESeq2' package, visualizing results with 'ggtreeExtra' (Xu *et al.*, 2021). To decipher the mechanisms underlying microbial community assembly, the βNTI (Beta Nearest Taxon Index) was computed using the 'picante' package (Mikryukov, 2019). This metric was integrated with the 'RCbray' index to jointly infer the relative contributions of deterministic and stochastic processes in the soil microbial community assembly. To identify key microbial taxa closely associated with plant biomass, random forest analysis was implemented using the 'randomForest' package and the significance of the model and cross-validated R2 values were assessed with 5000 permutations of the response variable by using the 'A3' package (Jiao *et al.*, 2018). The top 15 predictors (ASVs) most relevant to plant biomass were extracted for further analysis.

Co-occurrence networks were constructed for three interaction scenarios: intra-sexual interactions (females and males receiving same-sex exudates), inter-sexual interactions (females and males receiving opposite-sex exudates), and control (water-treated plants). Single-domain bacterial networks were inferred using SParse InversE Covariance Estimation for Ecological Association Inference (SpiecEasi) (Kurtz *et al.*, 2015). We utilized the

309 'glasso' method within the 'SpiecEasi' package, setting the lambda.min ratio to 0.05. Net-
310 work topology was calculated and visualized using the 'igraph' package, with node sizes
311 proportional to relative abundances. Topological parameters were compared between net-
312 works using Wilcoxon tests. For cross-kingdom (bacteria-fungi) networks, ASVs were first
313 filtered to include only those with >60% occurrence frequency across samples. Networks
314 were constructed using the 'ggClusterNet' package via the SparCC method (Wen *et al.*,
315 2022), retaining only robust correlations ($r > 0.8$, $p < 0.001$). To define the 'core network'
316 structure, all nodes lacking direct or indirect connections to the network's largest module
317 were removed; the remaining interconnected structure was analyzed as the core network.

Results

Responses to sex-specific soil microbial legacies

To test how *P. cathayana* responds to sex-specific soil microbial legacies, we firstly conducted a plant-soil feedback experiment (Fig. 1A and B). Although the total biomass and root architecture were not significantly affected by the soil legacy of either sex, we observed significant physiological changes (Fig. 1C-E). Specifically, females grown in foreign (male-conditioned) soil exhibited a significantly higher net photosynthetic rate and leaf N content compared to those in home (female-conditioned) soil. Similarly, males in foreign (female-conditioned) soil showed a higher root N content than males in home soil (Fig. 1D).

Sex-specific carbon allocation and microbiome recruitment

The $^{13}CO_2$ pulse-labeling experiment revealed sex-specific differences in carbon allocation to the rhizosphere microbiome. In females, the assimilation rate of new photosynthetic carbon by soil bacteria and fungi was similar between home and foreign soils (Fig. 2). In contrast, in males grown in foreign soil, the associated microbiome assimilated significantly more new photosynthetic carbon compared to that in home soil (Fig. 2). In female-conditioned soil, female plants enriched for Actinobacteria, Bacilli, and Agaricomycetes, whereas male plants enriched for Gammaproteobacteria and Bacteroidia (Fig. S3, S4). Male plants hosted a distinct and more diverse set of bacterial biomarkers in both soil types (Fig. S3, S4). Functionally, females in foreign soil induced a higher acid phosphatase (AP) activity, while males in foreign soil induced a higher β-1,4-glucosidase (BG) activity and increased soil N (Fig. S5).

Active foraging and carbon investment in a split-root system

To further explore belowground responses, we conducted a split-box experiment where plants could choose between male- and female-conditioned soils (Fig. 3A, B). While the traits of roots distributed into the home vs. foreign compartments were not significantly different in either sex (Fig. 3C-E), $^{13}CO_2$ tracing revealed a strong preferential allocation of carbon. Female plants allocated significantly more new photosynthates to microbes in the home soil compartment (Fig. 3H, I, K). Conversely, male plants allocated significantly more new carbon to all microbial groups in the foreign soil compartment (Fig. 3H-K).

Sex recognition via root exudates

To test the hypothesis that plants can chemically perceive the sexual identity of conspecifics, we designed a reciprocal transfer experiment (Fig. 4A and S1). Females had a higher biomass (Fig. 4B-E), higher leaf N and root N contents, and photosynthetic rate under inter-sexual interactions (Fig. 4F, J and L) than under intra-sexual interactions. Both sexes produced distinct root exudate profiles depending on neighbor identity (Fig. S6). In inter-sexual interactions, we identified 1025 differentially expressed metabolites (DEMs) up-regulated in females and 1169 DEMs up-regulated in males (Fig. 5E). In contrast, intra-sexual interactions yielded only 173 DEMs up-regulated in females and 632 DEMs up-regulated in males (Fig. 5F). The composition of these DEMs also differed markedly. Female exudates under inter-sexual conditions were enriched in certain flavonoids, whereas intra-sexual female exudates were characterized by defense-related compounds such as camalexin (Fig. S7, S8). KEGG pathway analysis further confirmed distinct functional signatures. Inter-sexual interactions primarily activated pathways associated with growth-related processes, including ubiquinone biosynthesis and sphingolipid signaling. In contrast, intra-sexual interactions predominantly triggered stress-response pathways, such as the biosynthesis of secondary metabolites and arginine metabolism (Fig. 5G, H).

Exudate-driven assembly of rhizosphere microbiome

To determine if sex-specific root exudates directly drive microbial community assembly, we applied different exudate solutions to plants established in their home soils (Fig. S2). Plants of each sex were exposed to three treatments: sterile water (Control), male root exudates (M-exu), or female root exudates (F-exu). Proteobacteria and Actinobacteriota were the dominant bacterial phyla across all rhizosphere samples (Fig. S9A). The relative abundance of an Ascomycota class was lower in plants receiving opposite-sex exudates compared to other treatments (Fig. S9B). In the male rhizosphere, the bacterial community in the M-exu treatment diverged significantly from both the Control and the F-exu treatments (Fig. S9C). In the female rhizosphere, however, both M-exu and F-exu treatments caused the bacterial community structure to shift significantly away from the Control group (Fig. S9D). In the male rhizosphere, both M-exu and F-exu treatments altered the fungal community structure compared to the Control (Fig. S9E), whereas the fungal community structure in the female rhizosphere showed no significant differences among the three treatments (Fig. S9F).

Community assembly processes and key taxa

In the female rhizosphere, β-Nearest Taxon Index (βNTI) values were similar across all treatments, suggesting consistent assembly processes (Fig. 6A). In contrast, in male plants, the βNTI value of the F-exu treatment was significantly higher than that in the other treatments, indicating a distinct shift in community assembly drivers (Fig. 6A). Notably, within the male rhizosphere, the community assembly drivers for plants receiving female exudates were different from those receiving male exudates. Compared to control, both same-sex and opposite-sex exudate applications led to a significant enrichment of distinct bacteria in both female and male rhizospheres (Fig. S10). A detailed analysis of these differentially enriched microbes revealed that exudate treatments induced highly treatment-specific ASV recruitment. In female plants, the F-exu treatment resulted in a distinct community profile, including many unique ASVs, compared to the M-exu treatment (Fig. 6B). Similarly, in male plants, a large number of ASVs were found exclusively in either the F-exu or M-exu

treatment, highlighting sex-specific microbial filtering (Fig. 6B). The Random forest analysis (R^2 = 62.9%, $P < 0.01$) identified key taxa being significantly associated with plant growth. Taxa belonging to the phyla Actinobacteriota and Proteobacteria were highly prevalent (Fig. 6C).

Network complexity and cross-kingdom interactions

We grouped the exudate treatments into three distinct categories: intra-sexual interactions (females and males receiving same-sex exudates), inter-sexual interactions (females and males receiving opposite-sex exudates, respectively), and control (water-treated plants). The co-occurrence analysis revealed that these three interaction types generated distinct bacterial network topologies (Fig. S11). The network derived from inter-sexual interactions featured a greater number of key topological nodes (12 connectors and 1 module hub) compared to the other networks (Fig. S11). This increased complexity with a significantly higher average node degree in the inter-sexual network, indicating a greater overall connectivity (Fig. S11). We extended this analysis to core cross-kingdom networks (bacteria-fungi). The inter-sexual interaction network was significantly larger, characterized by more nodes and edges (Fig. 7A). The composition of the taxa forming these networks was also distinct, and the phylogenetic diversity (PD) of these network members was significantly higher in the inter-sexual group (Fig. 7A-C). From control to intra-sexual to inter-sexual interactions, the relative abundance of Ascomycota decreased, while the relative abundance of Basidiomycota increased (Fig. 7D). Topologically, the inter-sexual cross-kingdom network showed a significantly higher closeness centrality (Fig. 7E). Furthermore, its core network structure contained a significantly higher proportion of positive edges than the other two treatments (Fig. 7F).

Discussion

Sex-specific legacies and physiological priming

While soil microbial legacies are increasingly recognized as drivers of ecosystem productivity and stumbling blocks for continuous poplar monocultures, our results revealed that these legacies are sexually distinct rather than neutral. *P. cathayana* females exhibited significantly higher net photosynthetic rates and leaf N contents when grown in male-conditioned soil compared to 'home' soil. This phenomenon likely represents a form of physiological priming, where plants living in favorable microbial environments prioritize nutrient acquisition and metabolic efficiency before allocating resources to structural growth. Sex-specific microbiota can be shaped by diverse dioecious species, which in turn affect their fitness in different environments (Vega-Frutis *et al.*, 2018; Guo *et al.*, 2022; Lin *et al.*, 2025). The underlying mechanism appears to be microbiome-mediated nutrient cycling. Previous research indicates that male and female poplars foster distinct microbial communities with divergent capacities for N cycling and phosphorus solubilization (Xia *et al.*, 2022; Guo *et al.*, 2024). Specifically, *P. euphratica* males typically maintain a higher abundance of phosphate-solubilizing bacteria (Xia *et al.*, 2022), and they show a higher net nitrification rate and BG activity compared to females (Guo *et al.*, 2024). Consequently, the microbial legacy in the male-conditioned soil appears to increase the bioavailability of limiting nutrients (e.g., nitrogen), which in turn promotes enhanced N uptake and photosynthetic performance in subsequent female individuals (Fig. 1). This implies that in natural or mixed-plantation settings, male plants may act as ‘soil conditioners’ that alleviate intraspecific competition in females, a critical ecological phenomenon related to the higher reproductive costs typically present in females.

Divergent carbon investment strategies in response to soil legacies

The input of root exudates fuels the survival, growth, and reproduction of soil microbes that form a direct communication pathway between the host and rhizosphere microbes (Zhalnina *et al.*, 2018). Our results showed that the pattern of carbon input depended on whether a plant is exposed to home or foreign soil, with consequences for microbial com-

munity composition and function. Our ^{13}C-labeling results revealed a clear sexual divergence in carbon allocation to the rhizosphere. It was observed that male plants allocated significantly more newly fixed photosynthates to soil bacteria and fungi when growing in foreign soil compared to home soil, whereas females did not exhibit such differential allocation (Fig. 2 and 3). This pattern aligns with known sexually dimorphic resource acquisition strategies in dioecious plants (Hultine *et al.*, 2016). Females, which typically bear high reproductive costs, may prioritize carbon conservation and exhibit more conservative belowground allocation under unfamiliar soil conditions (Xia *et al.*, 2022; Liu *et al.*, 2024). In contrast, males tend to maintain a stable root carbon sink to sustain their associated microbial partners and functions (Wu *et al.*, 2021; Xia *et al.*, 2022). By allocating significantly more new photosynthates to foreign soil, *P. cathayana* males were characterized by distinct microbial communities and elevated β-1,4-glucosidase activities (BG) (Fig. S3-S5). BG catalyzes the final step in cellulose degradation, hydrolyzing cellobiose to glucose monomers that can be rapidly assimilated by microbial cells (Bakshi & Varma, 2010). This enzyme activity exhibits strong positive correlations with the actively growing microbial biomass, indicating that an elevated BG activity specifically marks microsites where rapid carbon turnover and microbial proliferation occur (Kuzyakov & Blagodatskaya, 2015). These findings suggest that males can remodel the microbial community of foreign soils through increased labile carbon inputs, underscoring their role not merely as resource competitors, but as active modulators of soil microbial functioning.

Root exudates as a sex-specific chemical language

Previous studies have suggested that the sexual identity of neighbors differentially affects the growth of dioecious plants (Mercer & Eppley, 2014; Chen *et al.*, 2015; He *et al.*, 2021). Generally, female plants experience intense intraspecific competition when growing near same-sex neighbors, whereas inter-sexual interactions often facilitate resource use efficiency (Zhang *et al.*, 2021; Guo *et al.*, 2024). Consistently, our results confirmed that *P. cathayana* females grew significantly better, and exhibited higher N contents, photosynthetic rates and biomass, when exposed to male-conditioned solutions compared to female-conditioned solutions (Fig. 4). This distinct phenotypic plasticity demonstrates that plants

possess a capability for belowground sex recognition, utilizing the chemical composition of root exudates as a reliable informational cue to distinguish neighbors.

We found that this recognition drives a dynamic metabolic shift, orchestrating distinct strategies for competition versus facilitation. In intra-sexual interactions (female-female), plants upregulated potent defense-related compounds, such as antiarol and camalexin (Fig. 5). Camalexin, a major phytoalexin typically synthesized in response to a pathogen attack or competitive stress, can reshape microbial interactions in the rhizosphere by restricting the growth of sensitive bacterial competitors (Koprivova *et al.*, 2019). Since the biosynthesis of such secondary metabolites is energetically costly, their accumulation suggests that females perceive same-sex neighbors as competitive threats, triggering an active, high-cost defensive posture. This chemical stress response likely explains the lower biomass accumulation observed in same-sex pairs (Fig. 4). Conversely, inter-sexual interactions triggered a cooperative chemical dialogue that promoted female growth. On one hand, females responding to males specifically upregulated flavonoids (e.g., kaempferol 3-neohesperidoside) and phenolics. Flavonoids function as modulators of auxin transport and natural iron chelators, thereby enhancing root plasticity and nutrient mobility (Peer & Murphy, 2007; Cesco *et al.*, 2010). On the other hand, male exudates provided direct hormonal support; they were enriched in sorgolactone (a strigolactone analog) and gibberellin A59 (a gibberellin precursor) (Fig. S7). Strigolactones are well-documented to stimulate root hair elongation and mycorrhizal colonization (Kapulnik & Koltai, 2014), while gibberellins promote lateral root growth and overall root foraging capacity (van Gelderen *et al.*, 2025). Therefore, these growth signals promoted female root growth and N acquisition, and explain the superior photosynthetic performance of females in mixed-sex settings.

While previous research attributed the benefits of mixed-sex stands to spatial differentiation, such as males exploring deeper soil layers for water and N (Guo *et al.*, 2024), our study revealed an additional ‘chemical niche’ dimension. In monocultures, females with high nutrient demands suffer from severe niche overlap, leading to intense competition and stress-induced metabolic shifts. In mixed stands, however, the divergent exudate profiles

of males and females alleviate this competition. By shifting from defense (camalexin) to growth promotion (flavonoids/hormones), inter-sexual interactions optimize metabolic investments, driving the positive effects detected in this study. Although our experimental design did not directly test the causal effects of individual exudate compounds on microbial community shifts, the divergent metabolic profiles we observed under inter- versus intra-sexual interactions provide a mechanistic framework for future exudate-addition experiments for establishing direct chemical-microbiome linkages.

Sex-specific modulation of rhizosphere microbiome assembly

It is well-established that plant-mediated selective pressures, exerted through root exudation, determine the composition and function of the rhizosphere microbiota (Henneron *et al.*, 2020). In dioecious species, sexual dimorphism in exudate profiles is a crucial driver in shaping sex-specific microbial communities (He *et al.*, 2022; Guo *et al.*, 2024). Our findings confirm that the chemical plasticity of root exudates, triggered by neighbor identity, serves as a potent environmental filter that profoundly alters the rhizosphere microbiome, particularly the bacterial community (Fig. 6 and S9). We observed that male plants exhibited a stronger capacity to recruit unique bacterial ASVs and were more effective at modulating soil legacies than females (Fig. 6B and S10). Specifically, the male rhizosphere assembly was characterized by a higher influence of homogeneous selection when exposed to male exudates, suggesting a more deterministic and specialized recruitment process. This superior modulating ability in males is supported by our ^{13}C-labeling experiment, which revealed that males allocated significantly more newly fixed photosynthetic carbon to soil microbes in foreign soils compared to females (Fig. 2 and 3). While female carbon flow to the rhizosphere often decreases under stress due to a reduced photosynthetic capacity (He *et al.*, 2022; Liu *et al.*, 2024), males maintain a higher metabolic investment. This investment supports key taxa, such as Actinobacteriota, known for producing extracellular enzymes and antimicrobials, and Proteobacteria (particularly Gammaproteobacteria), which are metabolically versatile fast-growers linked to rapid nutrient cycling (Fig. 6) (Silva *et al.*, 2022; Ai *et al.*, 2025). Linked to previously reported higher acid phosphatase (AP) activities and stable phosphate-solubilizing communities reported in males (Xia *et*

al., 2024), our results underscore that male plants act as active modulators of soil legacies, capable of rapidly altering selective pressures to optimize the microbial environment.

Beyond altering community composition, the presence of neighbor-specific exudates imposes selective pressures that reshape microbe-microbe interactions. The preferential uptake of divergent metabolites leads to distinct microbial assemblages (Ulbrich *et al.*, 2022; Liu *et al.*, 2024). We found that inter-sexual interactions fostered more complex bacterial networks, characterized by a higher density of connectors, module hubs, and an increased average node degree (Fig. 7). Such highly interconnected networks, particularly those with enriched hub taxa, are known to enhance the resilience of microbial communities to environmental perturbations (Gao *et al.*, 2022). Notably, inter-sexual interactions also shaped a more complex cross-kingdom network with a higher phylogenetic diversity and a significantly greater proportion of positive edges compared to intra-sexual interactions (Fig. 7F). This shift suggests that inter-sexual dynamics facilitates cooperative microbial interactions rather than competition. The distinct exudate profiles of males and females under inter-sexual interactions likely create broader metabolic niches, reducing direct resource competition among microbial taxa and promoting niche complementarity. Males can improve female resistance to resource-limited environment by increasing water use-efficiency or nutrient uptake under inter-sexual interactions (Guo *et al.*, 2024; Liu *et al.*, 2024; Gao *et al.*, 2025). For example, the increased abundance of Basidiomycota in inter-sexual networks points to a transition toward more efficient ectomycorrhizal partnerships (Gao *et al.*, 2025). In these mixed-sex settings, males may facilitate N transport to females via common mycelial networks, a hypothesis supported by the significantly higher N content and improved physiological resistance observed in females under inter-sexual interactions observed in this study (Fig. 4). Collectively, these results demonstrate that while same-sex neighbors trigger competitive stress, inter-sexual chemical dialogues cultivate a cooperative and resilient soil microbiome that alleviates resource limitations.

This study establishes that *P. cathayana* possesses a sophisticated capacity for below-ground sex recognition, mediated by the metabolic plasticity of root exudates. Our findings

reveal a distinct sexual dimorphism in response strategies to neighbor identity. Females upregulated energetically costly compounds to counter intraspecific competition from same-sex neighbors, while shifting toward growth-promoting pathways and enhanced nutrient acquisition when perceiving male-derived cues. Males act as active soil conditioners, investing more newly fixed photosynthetic carbon into the soil to reshape microbial communities in ways that facilitate subsequent nutrient uptake by females. This male-driven carbon investment fosters more complex, cooperative cross-kingdom microbial networks, which mechanistically explains the improved nitrogen uptake and photosynthetic performance observed in females. From a silvicultural perspective, our results provide a mechanical basis for utilizing mixed-sex plantations to harness these natural sex-specific synergies, thereby enhancing ecosystem resilience and plantation productivity while mitigating the soil degradation common in single-sex monocultures.

Data availability: The raw sequence data reported in this paper have been deposited in the Genome Sequence Archive in National Genomics Data Center (Nucleic Acids Res 2025), China National Center for Bioinformation / Beijing Institute of Genomics, Chinese Academy of Sciences (GSA: CRA037748 and CRA037747) that are publicly accessible at https://ngdc.cncb.ac.cn/gsa.

Acknowledgments: We would like to thank students who gathered data, maintained plant experiments and collected samples from these experiments, especially Lin Liu, Fangyuan Sun and Yuanjing Zhu. This work was supported by the Hangzhou Natural Science Foundation (2025SZRJJ0048) and Talent Program of the Zhejiang University (0022112). We acknowledge that, during the preparation of this work, the authors used AI-assisted tools solely to improve grammatical clarity and enhance readability. The authors affirm that they take full responsibility for the content and scientific integrity of the publication.

Author Contributions: **Qingxue Guo**: Conceptualization; data curation; formal analysis; investigation; methodology; funding acquisition; project administration; visualization; writing-original draft. **Xinyi Chen and Jincheng Duan**: Data curation; investigation. **Helena Korpelainen**: Conceptualization; validation; writing-review and editing. **Chunyang Li**: Conceptualization; methodology; funding acquisition; project administration; resources; supervision; validation; writing - review and editing.

Competing Interest Statement: The authors declare no conflict of interest.

623 **References**

624 **Ai CF, He YQ, Cheng ZW, Wu JW, Liu C, Wang N, Yu Z, Liao HP, Zhou SG. 2025.** Unveiling
625 of active bacteria associated with nutrient cycling during cattle manure composting.
626 *Environmental Research* **286**: 122810.

627 **Bakshi M, Varma A 2010.** Soil enzyme: the state-of-art. *Soil enzymology*: Springer, 1–23.

628 **Beckers B, De Beeck MO, Thijs S, Truyens S, Weyens N, Boerjan W, Vangronsveld J. 2016.**
629 Performance of 16s rDNA Primer Pairs in the Study of Rhizosphere and Endosphere Bacterial
630 Microbiomes in Metabarcoding Studies. *Frontiers in Microbiology* **7**: 650.

631 **Cesco S, Neumann G, Tomasi N, Pinton R, Weisskopf L. 2010.** Release of plant-borne
632 flavonoids into the rhizosphere and their role in plant nutrition. *Plant and Soil* **329**: 1–25.

633 **Chen J, Dong TF, Duan BL, Korpelainen H, Niinemets Ü, Li CY. 2015.** Sexual competition and
634 N supply interactively affect the dimorphism and competiveness of opposite sexes in Populus
635 cathayana. *Plant Cell and Environment* **38**: 1285–1298.

636 **Fang LD, Ning QR, Guo JJ, Gong XW, Zhu JJ, Hao GY. 2021.** Hydraulic limitation underlies
637 the dieback of Populus pseudo-simonii trees in water-limited areas of northern China. *Forest*
638 *Ecology and Management* **483**: 118764.

639 **Frostegård Å, Bååth E, Tunlio A. 1993.** Shifts in the structure of soil microbial communities in
640 limed forests as revealed by phospholipid fatty acid analysis. *Soil Biology and Biochemistry* **25**:
641 723–730.

642 **Gao C, Xu L, Montoya L, Madera M, Hollingsworth J, Chen L, Purdom E, Singan V, Vogel**
643 **J, Hutmacher RB, et al. 2022.** Co-occurrence networks reveal more complexity than community
644 composition in resistance and resilience of microbial communities. *Nature Communications* **13**:
645 3867.

646 **Gao WT, Cisse EM, Khan Y, Li DD, Xu X. 2025.** Sex-Specific Root Strategies Drive Asymmetric
647 Nitrogen Transfer via Common Mycorrhizal Networks Under Nitrogen Deficiency in Populus
648 cathayana. *Plant Cell and Environment*: 1969–1979.

649 **Guo QX, Liu L, Liu JT, Korpelainen H, Li CY. 2022.** Plant sex affects plant-microbiome
650 assemblies of dioecious Populus cathayana trees under different soil nitrogen conditions.
651 *Microbiome* **10**: 191.

652 **Guo QX, Zhu YJ, Korpelainen H, Niinemets Ü, Li CY. 2023.** How does plant sex alter
653 microbiota assembly in dioecious plants? *Trends in Microbiology* **31**: 894–902.

654 **Guo QX, Zhu YJ, Sun FY, Korpelainen H, Niinemets Ü, Li CY. 2024.** Male, female, and mixed-
655 sex poplar plantations support divergent soil microbial communities. *Global Change Biology* **30**:

e17198.

Hannula SE, Heinen R, Huberty M, Steinauer K, De Long JR, Jongen R, Bezemer TM. 2021. Persistence of plant-mediated microbial soil legacy effects in soil and inside roots. *Nature Communications* **12**: 5686.

He Y, Zhu ZD, Zhou ZH, Lu T, Kumar A, Xia ZC. 2022. Foliar application of lambda-cyhalothrin modulates root exudate profile and the rhizosphere bacteria community of dioecious Populus cathayana. *Environmental Pollution* **313**: 120123.

He YL, Xu H, Liu HL, Luo ML, Chu CJ, Fang SQ. 2021. Sexual competition and kin recognition co-shape the traits of neighboring dioecious Diospyros morrisiana seedlings. *Horticulture Research* **8**: 162.

Henneron L, Kardol P, Wardle DA, Cros C, Fontaine S. 2020. Rhizosphere control of soil nitrogen cycling: a key component of plant economic strategies. *New Phytologist* **228**: 1269–1282.

Hultine KR, Grady KC, Wood TE, Shuster SM, Stella JC, Whitham TG. 2016. Climate change perils for dioecious plant species. *Nature Plants* **2**: 16109.

Jiao S, Chen WM, Wang JL, Du NN, Li QP, Wei GH. 2018. Soil microbiomes with distinct assemblies through vertical soil profiles drive the cycling of multiple nutrients in reforested ecosystems. *Microbiome* **6**: 146.

Jing H, Wang HL, Wang GL, Liu GB, Cheng Y. 2023. The mechanism effects of root exudate on microbial community of rhizosphere soil of tree, shrub, and grass in forest ecosystem under N deposition. *Isme Communications* **3**: 120.

Jing X, Chen X, Fang JY, Ji CJ, Shen HH, Zheng CY, Zhu B. 2020. Soil microbial carbon and nutrient constraints are driven more by climate and soil physicochemical properties than by nutrient addition in forest ecosystems. *Soil Biology & Biochemistry* **141**: 107657.

Joergensen RG. 2022. Phospholipid fatty acids in soil-drawbacks and future prospects. *Biology and Fertility of Soils* **58**: 1–6.

Kapulnik Y, Koltai H. 2014. Strigolactone Involvement in Root Development, Response to Abiotic Stress, and Interactions with the Biotic Soil Environment. *Plant Physiology* **166**: 560–569.

Kong CH, Zhang SZ, Li YH, Xia ZC, Yang XF, Meiners SJ, Wang P. 2018. Plant neighbor detection and allelochemical response are driven by root-secreted signaling chemicals. *Nature Communications* **9**: 3867.

Koprivova A, Schuck S, Jacoby RP, Klinkhammer I, Welter B, Leson L, Martyn A, Nauen J,

Grabenhorst N, Mandelkow JF, et al. 2019. Root-specific camalexin biosynthesis controls the plant growth-promoting effects of multiple bacterial strains. *Proceedings of the National Academy of Sciences of the United States of America* **116**: 15735–15744.

Kurtz ZD, Müller CL, Miraldi ER, Littman DR, Blaser MJ, Bonneau RA. 2015. Sparse and Compositionally Robust Inference of Microbial Ecological Networks. *Plos Computational Biology* **11**: e1004226.

Kuzyakov Y, Blagodatskaya E. 2015. Microbial hotspots and hot moments in soil: Concept & review. *Soil Biology & Biochemistry* **83**: 184–199.

Lin CF, Wu JJ, Zhao YP. 2025. Host-mediated selection drives sexual dimorphism of microbiota assembly in the dioecious living fossil Ginkgo biloba. *New Phytologist* **248**: 3208–3220.

Liu C, Cui YM, Li XZ, Yao MJ. 2021. microeco: an R package for data mining in microbial community ecology. *Fems Microbiology Ecology* **97**: fiaa255.

Liu JT, Sun FY, Yu YN, Guo QX. 2024. The sexual identity of neighboring plants influences root-associated bacteria under drought. *Plant and Soil L* **497**: 669–685.

Luo J, Zhou J, Li H, Shi WG, Polle A, Lu MZ, Sun XM, Luo ZB. 2015. Global poplar root and leaf transcriptomes reveal links between growth and stress responses under nitrogen starvation and excess. *Tree Physiology* **35**: 1283–1302.

Luo RY, Kuzyakov Y, Zhu B, Qiang W, Zhang Y, Pang XY. 2022. Phosphorus addition decreases plant lignin but increases microbial necromass contribution to soil organic carbon in a subalpine forest. *Global Change Biology* **28**: 4194–4210.

Mao YF, Li N, Huang YL, Chen DW, Sun K. 2024. Divergence of rhizosphere microbial communities between females and males of the dioecious Hippophae tibetana at different habitats. *Microbiology Spectrum* **12**: e01670–01624.

McKay GJ, Brown AE, Bjourson AJ, Mercer PC. 1999. Molecular characterisation of Alternaria linicola and its detection in linseed. *European Journal of Plant Pathology* **105**: 157–166.

Mercer CA, Eppley SM. 2014. Kin and sex recognition in a dioecious grass. *Plant Ecology* **215**: 845–852.

Mikryukov V 2019. Miscellaneous functions for metagenomic analysis.

Moutouama JK, Compagnoni A, Miller TEX. 2025. Forecasting range shifts of dioecious plants under climate change. *Proceedings of the National Academy of Sciences of the United States of America* **122**: e2422162122.

Nannipieri P, Hannula SE, Pietramellara G, Schloter M, Sizmur T, Pathan SI. 2023. Legacy effects of rhizodeposits on soil microbiomes: A perspective. *Soil Biology & Biochemistry* **184**:

109107.

Peer WA, Murphy AS. 2007. Flavonoids and auxin transport: modulators or regulators? *Trends in Plant Science* **12**: 556–563.

Ren ZB, Xing CW, Li YN, Ma ZW, Gu JC. 2021. Features of vegetation community and physicochemical properties of soil during natural restoration in destoration grassland. *Journal of Environmental Protection and Ecology* **22**: 132–144.

Renner SS. 2014. The relative and absolute frequencies of angiosperm sexual systems: dioecy, monoecy, gynodioecy, and an updated online database. *American Journal of Botany* **101**: 1588–1596.

Schindlbacher A, Rodler A, Kuffner M, Kitzler B, Sessitsch A, Zechmeister-Boltenstern S. 2011. Experimental warming effects on the microbial community of a temperate mountain forest soil. *Soil Biology & Biochemistry* **43**: 1417–1425.

Silva GD, Kitano IT, Ribeiro IAD, Lacava PT. 2022. The Potential Use of Actinomycetes as Microbial Inoculants and Biopesticides in Agriculture. *Frontiers in Soil Science* **2**: 833181.

Sloan S, Sayer JA. 2015. Forest Resources Assessment of 2015 shows positive global trends but forest loss and degradation persist in poor tropical countries. *Forest Ecology and Management* **352**: 134–145.

Thornton B, Zhang ZL, Mayes RW, Högberg MN, Midwood AJ. 2011. Can gas chromatography combustion isotope ratio mass spectrometry be used to quantify organic compound abundance? *Rapid Communications in Mass Spectrometry* **25**: 2433–2438.

Ulbrich TC, Rivas-Ubach A, Tiemann LK, Friesen ML, Evans SE. 2022. Plant root exudates and rhizosphere bacterial communities shift with neighbor context. *Soil Biology & Biochemistry* **172**: 108753.

van Gelderen K, van der Velde K, Kang CK, Hollander J, Koppenol A, Petropoulos O, Prasetyaningrum P, Akyüz T, Pierik R. 2025. Gibberellin transport affects lateral root growth through HY5 in response to far-red light. *Plant Cell* **37**: koaf200.

Vega-Frutis R, Luna-Esquivel G, Figueroa-Esquivel EM. 2018. Land-use change impact on mycorrhizal symbiosis in female and male plants of wild Carica papaya (Caricaceae). *Symbiosis* **76**: 209–219.

Wen T, Xie PH, Yang SD, Niu GQ, Liu XY, Ding ZX, Xue C, Liu YX, Shen QR, Yuan J. 2022. ggClusterNet: An R package for microbiome network analysis and modularity-based multiple network layouts. *Imeta* **1**: e32.

White DC, Davis WM, Nickels JS, King JD, Bobbie RJ. 1979. Determination of the sedimentary

755 microbial biomass by extractible lipid phosphate. *Oecologia* **40**: 51–62.
756 **Willers C, van Rensburg PJJ, Claassens S. 2015.** Phospholipid fatty acid profiling of microbial
757 communities-a review of interpretations and recent applications. *Journal of Applied*
758 *Microbiology* **119**: 1207–1218.
759 **Wu XY, Liu JT, Meng QQ, Fang SY, Kang JY, Guo QX. 2021.** Differences in carbon and
760 nitrogen metabolism between male and female Populus cathayana in response to deficient
761 nitrogen. *Tree Physiology* **41**: 119–133.
762 **Xia ZC, Chen BJW, Korpelainen H, Niinemets Ü, Li CY. 2024.** Belowground ecological
763 interactions in dioecious plants: why do opposites attract but similar ones repel? *Trends in Plant*
764 *Science* **29**: 630–637.
765 **Xia ZC, He Y, Korpelainen H, Niinemets Ü, Li CY. 2023.** Allelochemicals and soil
766 microorganisms jointly mediate sex-specific belowground interactions in dioecious Populus
767 cathayana. *New Phytologist* **240**: 1519–1533.
768 **Xia ZC, He Y, Zhu ZD, Korpelainen H, Li CY. 2022.** Covariations and trade-offs of phosphorus
769 (P) acquisition strategies in dioecious Populus euphratica as affected by soil water availability.
770 *Functional Ecology* **36**: 3188–3199.
771 **Xu SB, Dai ZH, Guo PF, Fu XC, Liu SS, Zhou L, Tang WL, Feng TZ, Chen MJ, Zhan L, et**
772 **al. 2021.** ggtreeExtra: Compact Visualization of Richly Annotated Phylogenetic Data. *Molecular*
773 *Biology and Evolution* **38**: 4039–4042.
774 **Zhalnina K, Louie KB, Hao Z, Mansoori N, da Rocha UN, Shi SJ, Cho HJ, Karaoz U, Loqué**
775 **D, Bowen BP, et al. 2018.** Dynamic root exudate chemistry and microbial substrate preferences
776 drive patterns in rhizosphere microbial community assembly. *Nature Microbiology* **3**: 470–480.
777 **Zhang CY, Zhu J, Liu G, Huang YY, Huang GQ, Xu X. 2021.** The sexual dimorphism displayed
778 by the roots of mulberry (Morus alba) saplings depends on the sex of the neighboring plants.
779 *Journal of Plant Ecology* **14**: 1037–1046.
780 **Zhang YY, Zheng NG, Wang J, Yao HY, Qiu QF, Chapman SJ. 2019.** High turnover rate of free
781 phospholipids in soil confirms the classic hypothesis of PLFA methodology. *Soil Biology &*
782 *Biochemistry* **135**: 323–330.

Figure legends

Figure 1. Physiological responses of *P. cathayana* to sex-specific soil microbial legacies. (A) Schematic presentation of the soil conditioning phase generating female- and male-conditioned soils. **(B)** Experimental design involving window rhizoboxes with four treatment combinations (n=5): females grown in female-conditioned ('home') or male-conditioned ('foreign') soil, and males grown in female-conditioned ('foreign') or male-conditioned ('home') soil. **(C-E)** Comparison of plant biomass and root architecture between home (red bars) and foreign (blue bars) soil conditions. Data are mean ± SE. Asterisks indicate significant differences according to Student's *t*-test (*ns*, not significant; *, $0.01<P\leq0.05$; **, $0.001<P\leq0.01$.).

Figure 2. Sex-specific carbon allocation to the rhizosphere microbiome revealed by $^{13}CO_2$ pulse-labeling. The relative abundance of ^{13}C assimilated by soil microbes is shown for female and male plants grown in home versus foreign soils (n=5). Red bars represent home soil; blue bars represent foreign soil. Statistical significance was determined by Student's *t*-test (*ns*, not significant; *, $0.01<P\leq0.05$; **, $0.001<P\leq0.01$.).

Figure 3. Active foraging and preferential carbon investment in a split-root soil choice experiment (n=5)**. (A-B)** Schematic presentation of the split-root system where individual plants had simultaneous access to both female- and male-conditioned soil compartments. **(C-F)** Root morphological traits and soil N in each soil compartment. **(G-K)** Allocation of 1^3C-labeled photosynthates to microbial groups in each compartment. ns, no significant difference; *, $0.01<P\leq0.05$; **, $0.001<P\leq0.01$; *** $P\leq0.001$.

Figure 4. Physiological evidence of belowground sex recognition in a hydroponic reciprocal transfer system. (A) Schematic presentation of the experimental design. Plants were reciprocally transferred between hydroponic solutions conditioned by either same-sex or opposite-sex roots every 24 h (n=5). **(B-E)** Total biomass and allocation patterns of

female and male plants in intra-sexual (female-female, male-male) versus inter-sexual (female-male) interactions. **(F-L)** Leaf physiological traits including net photosynthetic rate (P_n), and nitrogen content. Data are mean ± SE. Tukey's test was used for multiple comparisons. Different letters indicate significant differences at $P \leq 0.05$.

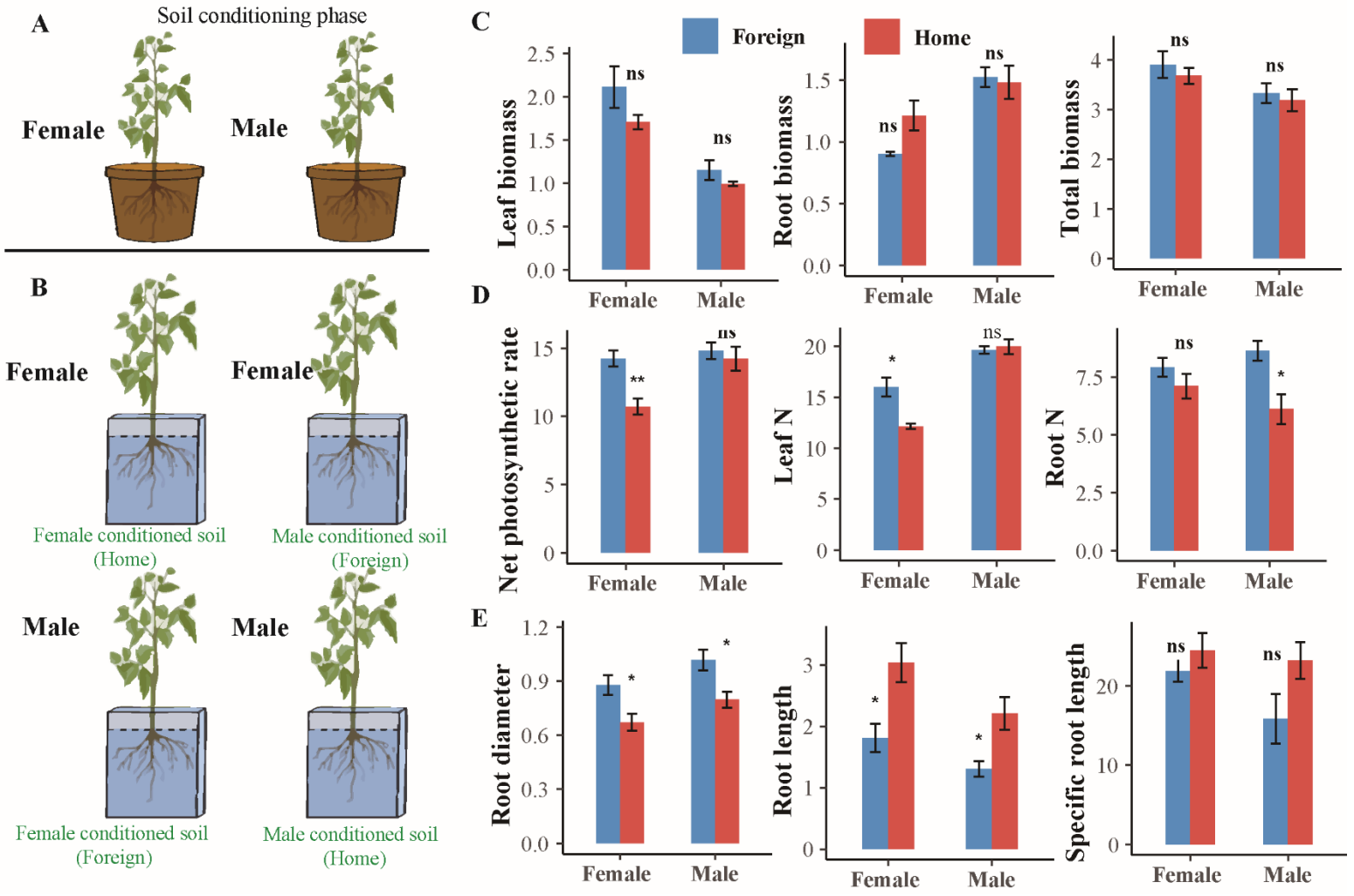
Figure 5. Chemotaxonomic profiling and functional pathways of root exudates modulated by neighbor identity. (A-B) The OPLS-DA analysis of root exudates between males and females under inter- and intra-sexual interactions, respectively. **(C)** The composition and proportion of root exudates under inter-sexual interactions. **(D)** The composition and proportion of root exudates under intra-sexual interactions. **(E)** The volcano plot of root exudate profiles from inter-sexual interactions. The green dots indicate DMEs enriched in males, while the orange dots indicate DMEs enriched in females. **(F)** The volcano plot of root exudate profiles from intra-sexual interactions. The green dots indicate DMEs enriched in males, while the orange dots indicate DMEs enriched in females. **(G)** KEGG functions of DMEs between females and males identified from inter-sexual interactions. **(H)** KEGG functions of DMEs between females and males identified from intra-sexual interactions. The size of circles shows the abundance of DMEs in each function pathway. The color of each circle shows *P* values.

Figure 6. Rhizosphere microbiome assembly driven by sex-specific root exudates. (A) Beta-Nearest Taxon Index (βNTI) indicating the relative importance of deterministic vs. stochastic assembly processes (n=5). **(B)** Phylogenetic tree of different enriched and depleted bacterial ASVs. These ASVs were identified by DESeq2 analysis in Figure S9. The blue and orange color within the first inner ring shows depleted and enriched ASVs, respectively, while the color gradients show Log_2 Fold Change. The circle and star shapes

represent unique and shared ASVs, respectively. (C) Top 15 ASVs most relevant to plant biomass identified by random forest analysis.

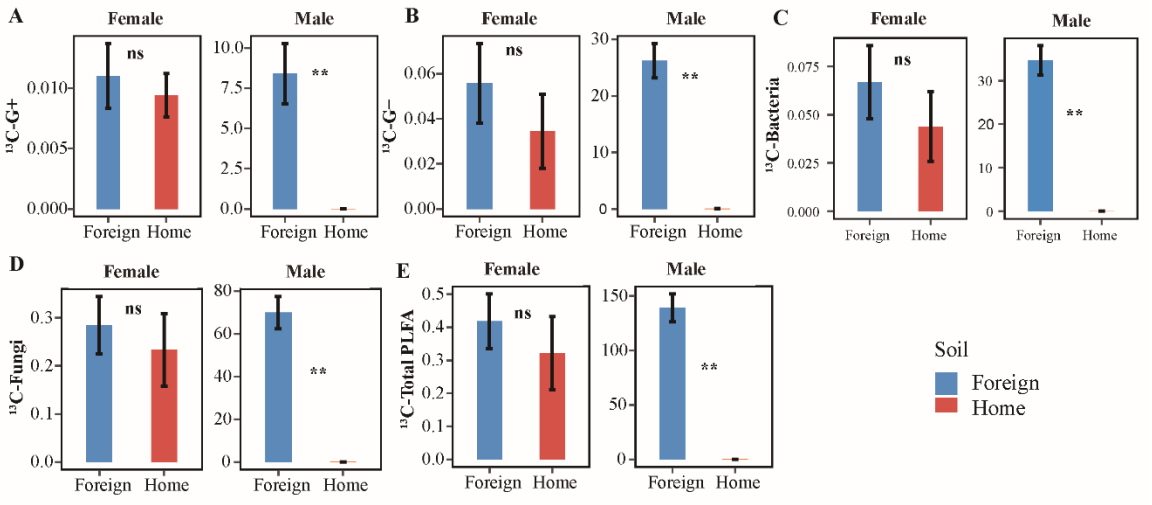
Figure 7. Topology and composition of core cross-kingdom (bacterial-fungal) co-occurrence networks. (A) Topological properties of networks constructed under three interaction scenarios: intra-sexual (plants receiving same-sex exudates, n=10), inter-sexual (plants receiving opposite-sex exudates, n=10), and control (water-treated plants, n=10). In network diagrams, solid circles represent bacterial ASVs, solid squares represent fungal ASVs, and node colors correspond to microbial phyla. **(B)** Principal Coordinate Analysis (PCoA) of bacterial and fungal communities across treatments. **(C)** Alpha diversity indices (Shannon, Simpson) and phylogenetic diversity (PD) of ASVs within the core networks. **(D)** Taxonomic composition and relative abundance of ASVs within each network. **(E-F)** Topological properties of networks.

849 **Figure 1**

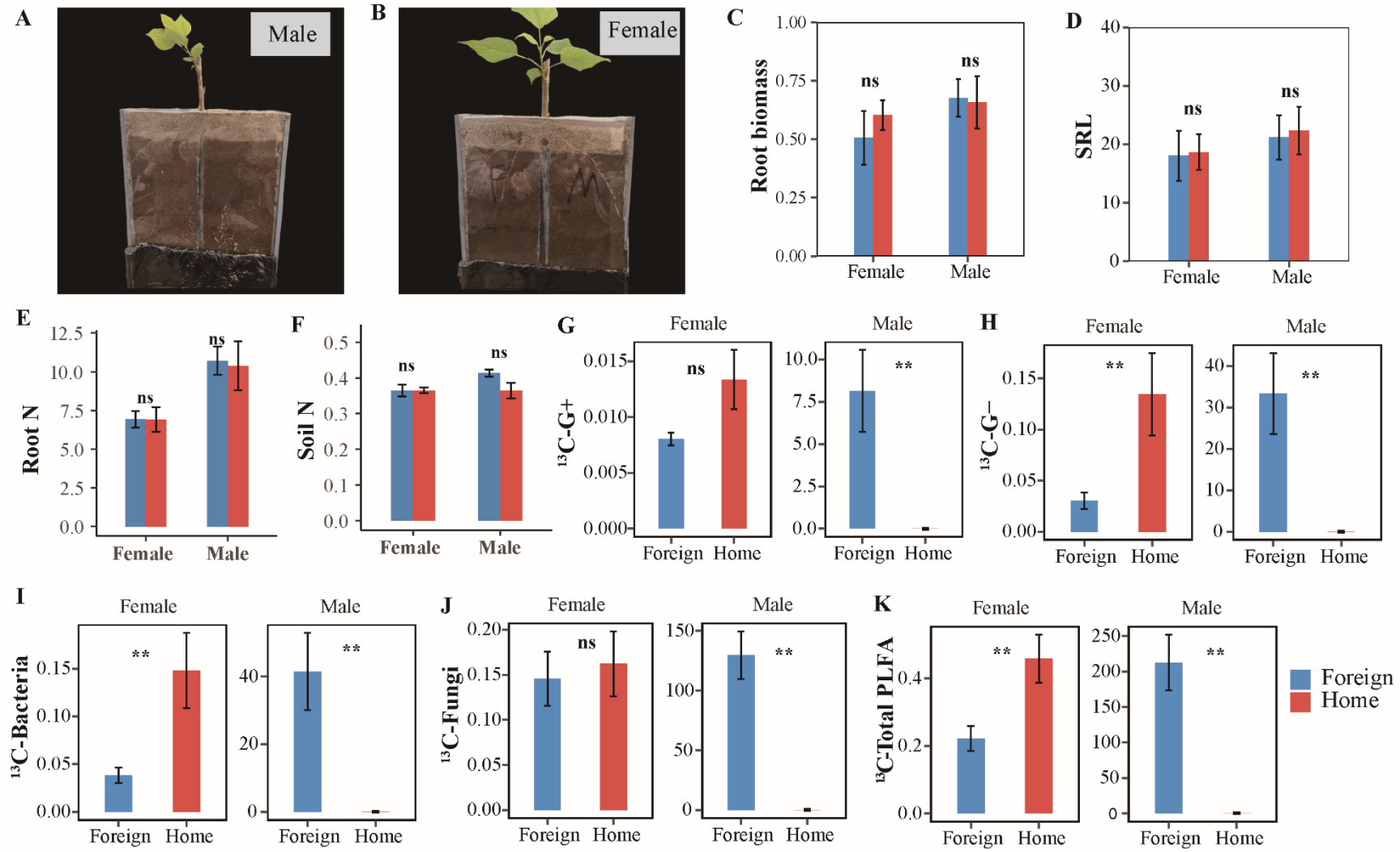


850

Figure 2


A
Female
Male
ns
**
^{13}C-G+
B
^{13}C-G−
C
^{13}C-Bacteria
D
^{13}C-Fungi
E
^{13}C-Total PLFA
Foreign
Home
Soil
Foreign
Home

853 **Figure 3**



854

Figure 4

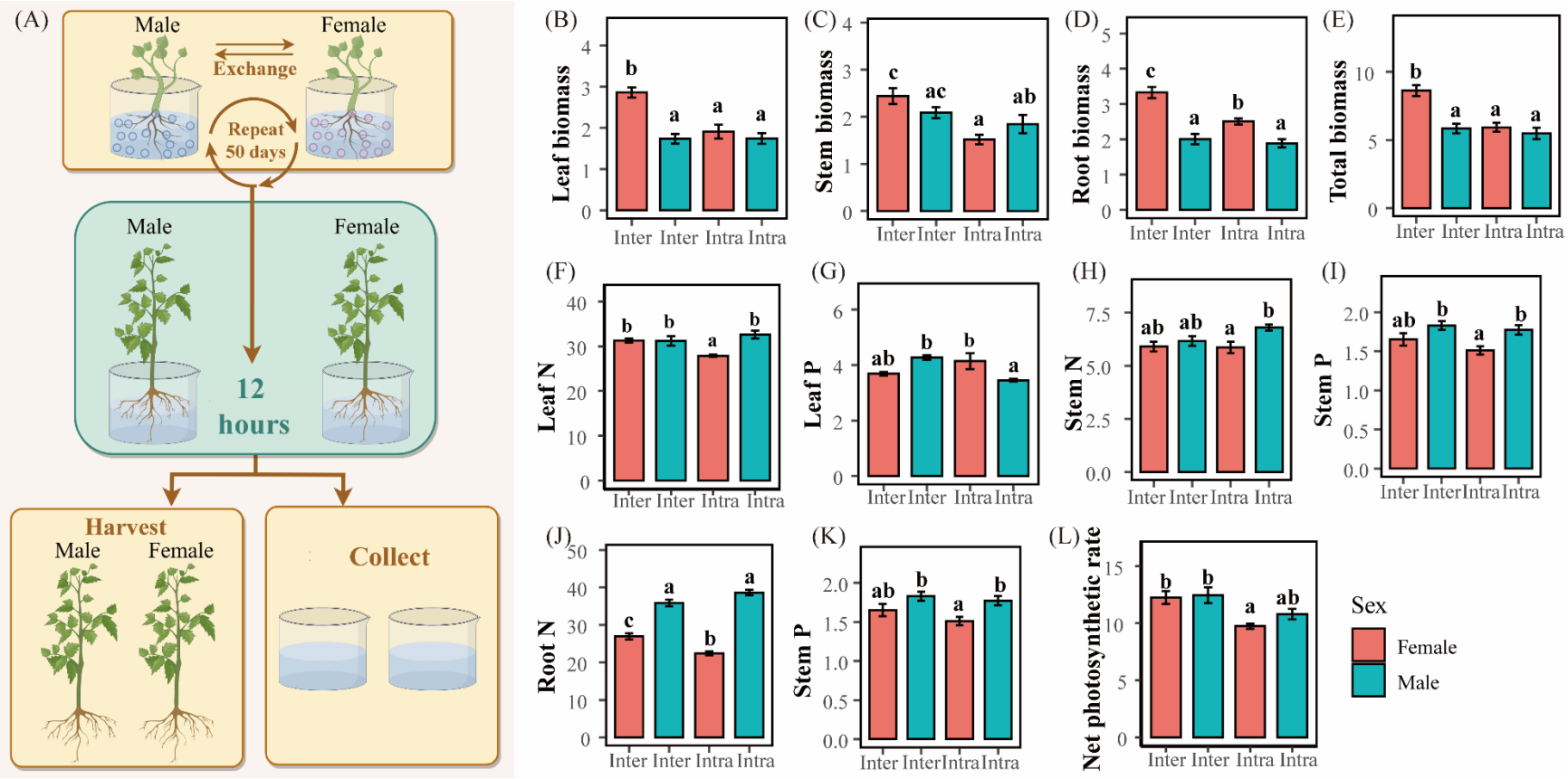

(A)
Male
Female
Exchange
Repeat
50 days
Male
Female
12
hours
Harvest
Male
Female
Collect
(B)
Leaf biomass
(C)
Stem biomass
(D)
Root biomass
(E)
Total biomass
(F)
Leaf N
(G)
Leaf P
(H)
Stem N
(I)
Stem P
(J)
Root N
(K)
Stem P
(L)
Net photosynthetic rate
Inter Inter Intra Intra
Sex
Female
Male

Figure 5

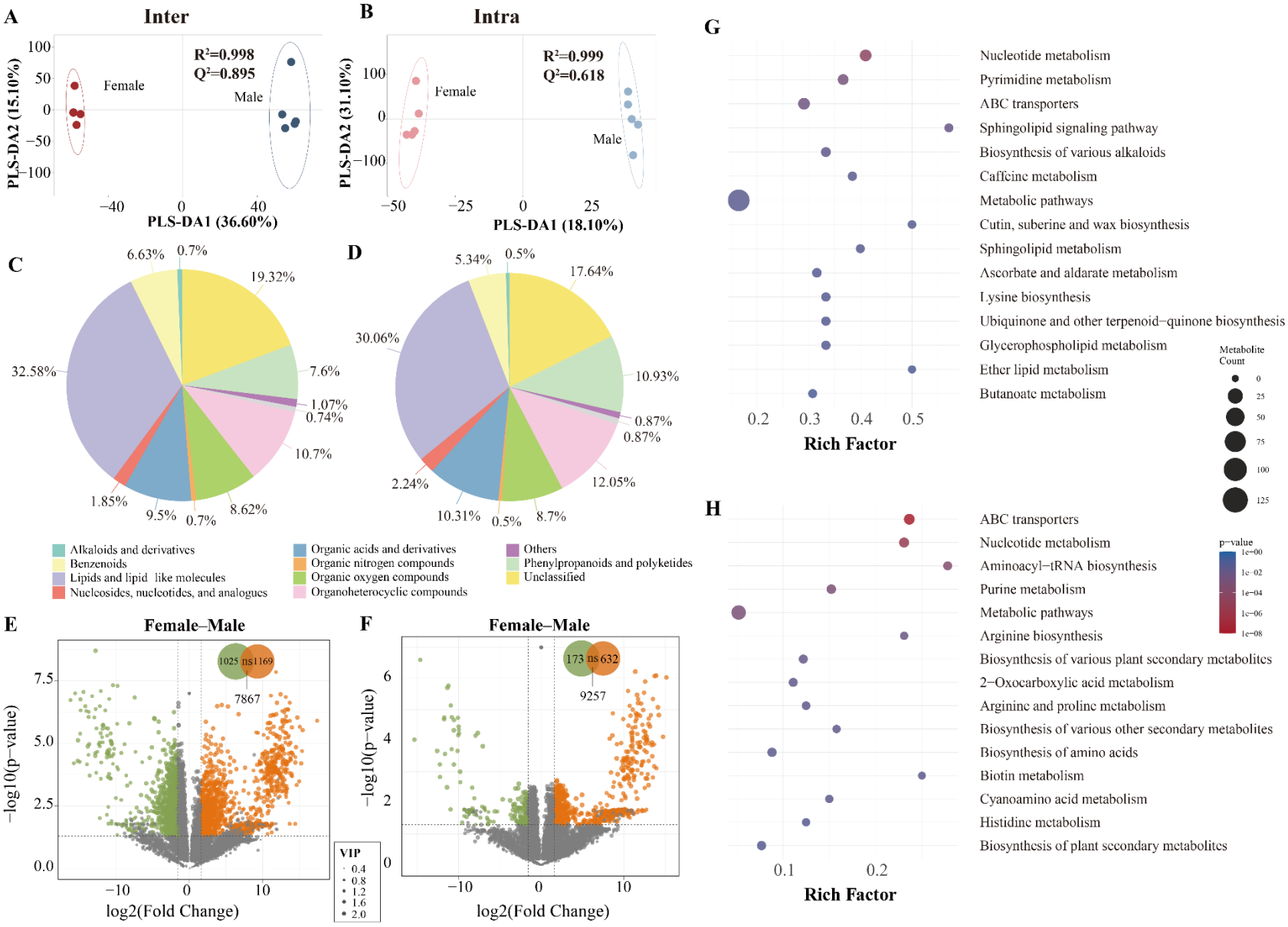

A
Inter
R²=0.998
Q²=0.895
Female
Male
PLS-DA2 (15.10%)
PLS-DA1 (36.60%)
B
Intra
R²=0.999
Q²=0.618
Female
Male
PLS-DA2 (31.10%)
PLS-DA1 (18.10%)
C
6.63%
0.7%
19.32%
7.6%
1.07%
0.74%
10.7%
8.62%
0.7%
9.5%
1.85%
32.58%
D
5.34%
0.5%
17.64%
10.93%
0.87%
0.87%
12.05%
8.7%
0.5%
10.31%
2.24%
30.06%
Alkaloids and derivatives
Benzenoids
Lipids and lipid like molecules
Nucleosides, nucleotides, and analogues
Organic acids and derivatives
Organic nitrogen compounds
Organic oxygen compounds
Organoheterocyclic compounds
Others
Phenylpropanoids and polyketides
Unclassified
E
Female–Male
1025
ns
1169
7867
−log10(p−value)
log2(Fold Change)
VIP
0.4
0.8
1.2
1.6
2.0
F
Female–Male
173
ns
632
9257
−log10(p−value)
log2(Fold Change)
G
Nucleotide metabolism
Pyrimidine metabolism
ABC transporters
Sphingolipid signaling pathway
Biosynthesis of various alkaloids
Caffeine metabolism
Metabolic pathways
Cutin, suberine and wax biosynthesis
Sphingolipid metabolism
Ascorbate and aldarate metabolism
Lysine biosynthesis
Ubiquinone and other terpenoid−quinone biosynthesis
Glycerophospholipid metabolism
Ether lipid metabolism
Butanoate metabolism
Rich Factor
Metabolite Count
H
ABC transporters
Nucleotide metabolism
Aminoacyl−tRNA biosynthesis
Purine metabolism
Metabolic pathways
Arginine biosynthesis
Biosynthesis of various plant secondary metabolites
2−Oxocarboxylic acid metabolism
Arginine and proline metabolism
Biosynthesis of various other secondary metabolites
Biosynthesis of amino acids
Biotin metabolism
Cyanoamino acid metabolism
Histidine metabolism
Biosynthesis of plant secondary metabolites
Rich Factor
p−value

Figure 6

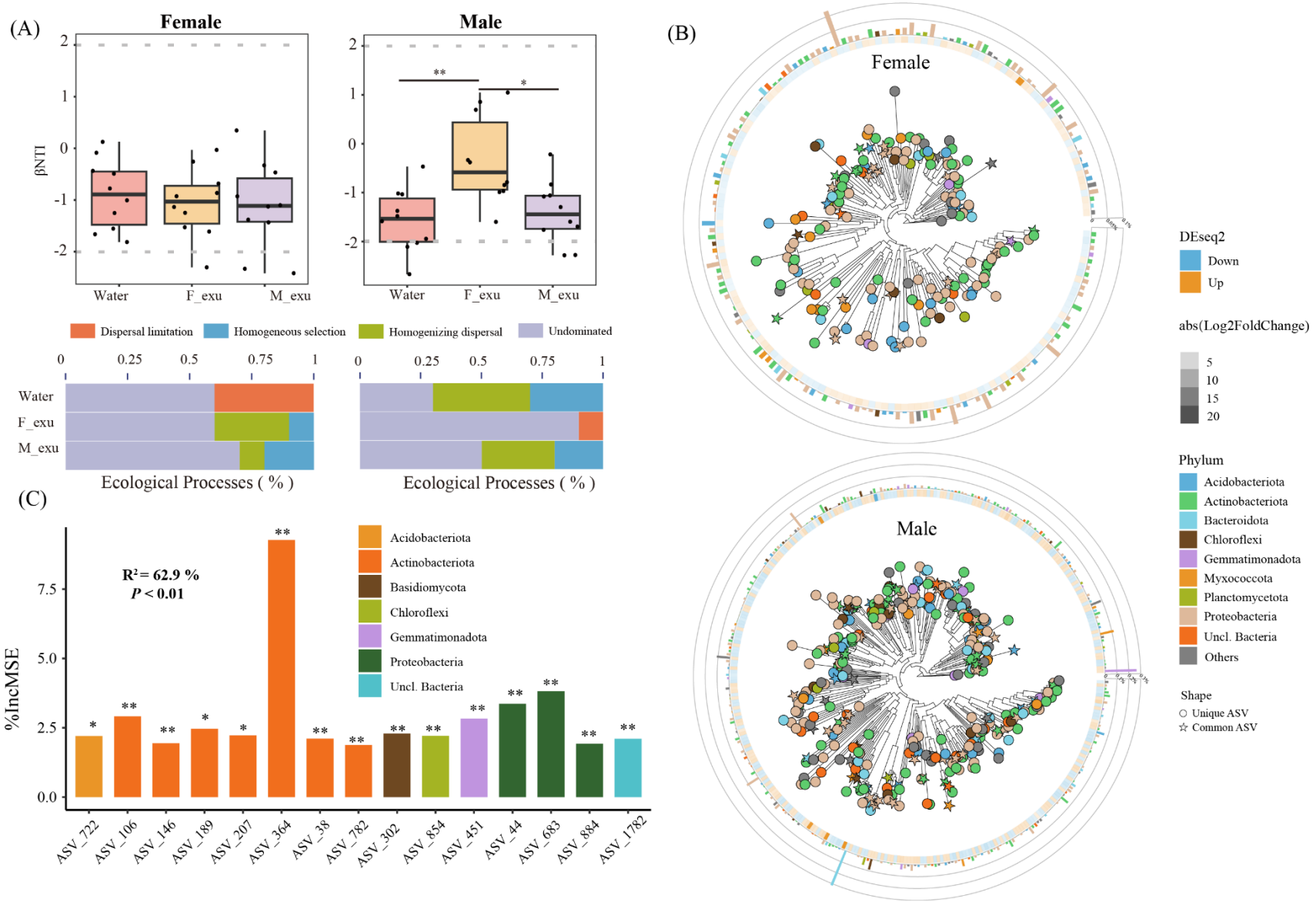
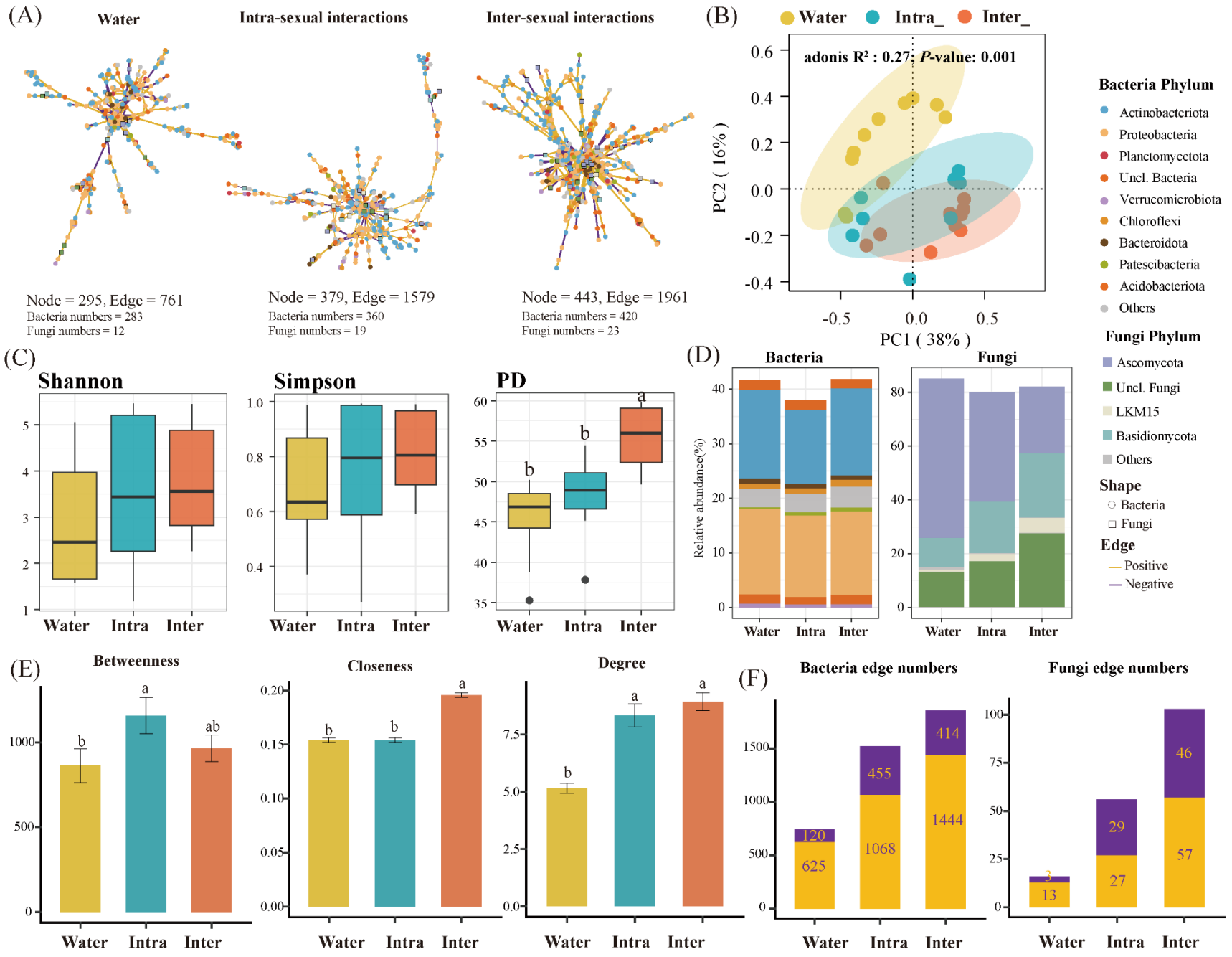

(A)
Female
Male
βNTI
Water
F_exu
M_exu
Dispersal limitation
Homogeneous selection
Homogenizing dispersal
Undominated
Ecological Processes (%)
(B)
Female
Male
DEseq2
Down
Up
abs(Log2FoldChange)
Phylum
Acidobacteriota
Actinobacteriota
Bacteroidota
Chloroflexi
Gemmatimonadota
Myxococcota
Planctomycetota
Proteobacteria
Uncl. Bacteria
Others
Shape
Unique ASV
Common ASV
(C)
R² = 62.9 %
P < 0.01
%IncMSE
Basidiomycota
ASV_722
ASV_106
ASV_146
ASV_189
ASV_207
ASV_364
ASV_38
ASV_782
ASV_302
ASV_854
ASV_451
ASV_44
ASV_683
ASV_884
ASV_1782

Figure 7


(A)
Water
Intra-sexual interactions
Inter-sexual interactions
Node = 295, Edge = 761
Bacteria numbers = 283
Fungi numbers = 12
Node = 379, Edge = 1579
Bacteria numbers = 360
Fungi numbers = 19
Node = 443, Edge = 1961
Bacteria numbers = 420
Fungi numbers = 23
(B)
Water
Intra_
Inter_
adonis R² : 0.27; P-value: 0.001
PC2 (16%)
PC1 (38%)
Bacteria Phylum
Actinobacteriota
Proteobacteria
Planctomycetota
Uncl. Bacteria
Verrucomicrobiota
Chloroflexi
Bacteroidota
Patescibacteria
Acidobacteriota
Others
Fungi Phylum
Ascomycota
Uncl. Fungi
LKM15
Basidiomycota
Others
Shape
Bacteria
Fungi
Edge
Positive
Negative
(C)
Shannon
Simpson
PD
Water
Intra
Inter
(D)
Bacteria
Fungi
Relative abundance(%)
(E)
Betweenness
Closeness
Degree
(F)
Bacteria edge numbers
Fungi edge numbers
120
625
455
1068
414
1444
3
13
29
27
46
57